We are IntechOpen, the world's leading publisher of Open Access books Built by scientists, for scientists

4,800
Open access books available

122,000
International authors and editors

135M
Downloads

Our authors are among the

154
Countries delivered to

TOP 1%
most cited scientists

12.2%
Contributors from top 500 universities

CLARIVATE ANALYTICS BOOK CITATION INDEX INDEXED

WEB OF SCIENCE™

Selection of our books indexed in the Book Citation Index in Web of Science™ Core Collection (BKCI)

Interested in publishing with us?
Contact book.department@intechopen.com

Numbers displayed above are based on latest data collected.
For more information visit www.intechopen.com

7

Fully Printable Chipless RFID Tag

Stevan Preradovic and Nemai Karmakar
Monash University
Australia

1. Introduction

1.1 Radio frequency identification

Radio frequency identification (RFID) is a wireless data capturing technique which utilizes radio frequency (RF) waves for automatic identification of objects. RFID relies on RF waves for data transmission between the data carrying device, called the RFID tag, and the interrogator (Finkenzeller, 2003; Kraiser & Steinhagen, 1995)

A typical RFID system is shown in Fig. 1. An RFID system consists of three major components: a **reader** or **interrogator**, which sends the interrogation signals to an RFID tag, which is to be identified; an RFID **tag** or **transponder**, which contains the identification code; and **middleware software**, which maintains the interface and the software protocol to encode and decode the identification data from the reader into a mainframe or personal computer. The RFID reader can read tags only within the reader's interrogation zone. The reader is most commonly connected to a host computer which performs additional signal processing and has a display of the tag's identity (Preradovic & Karmakar, 2007). The host computer can also be connected via internet for global connectivity/networking.

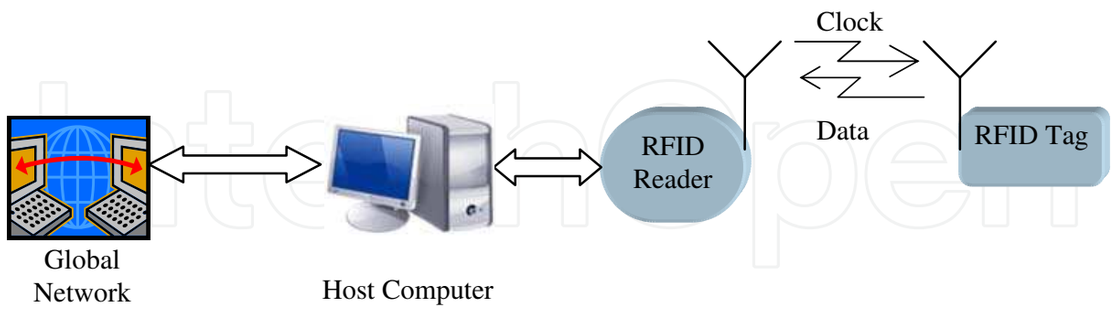

Fig. 1. Block diagram of a typical RFID system.

RFID was first proposed by Stockman (Stockman, 1948) in his landmark paper "Communication by Means of Reflected Power" in 1948. Stockman advocates that by alternating the load of the tag antenna it is possible to vary the amount of reflected power (also called "antenna load modulation") and therefore perform modulation. This new form of wireless technology is now known as RFID. Since then researchers and engineers have been working on developing low cost RFID systems.

1.2 Difficulties of achieving low cost RFID

The use of RFID instead of optical barcodes has not yet been achieved due to the greater price of the RFID tag (10 cents) compared to the price of the optical barcode (less than 0.1 cents). The arguments for not having a cheap RFID tag are comprehensively presented in (Fletcher, 2002). Fletcher advocates that Application Specific Integrated Circuit (ASIC) design and testing along with the tag antenna and ASIC assembly result in a costly manufacturing process. This is why it is not possible to further lower the price of the chipped RFID tag. The basic steps for manufacturing a chipped RFID tag are shown in Fig 2.

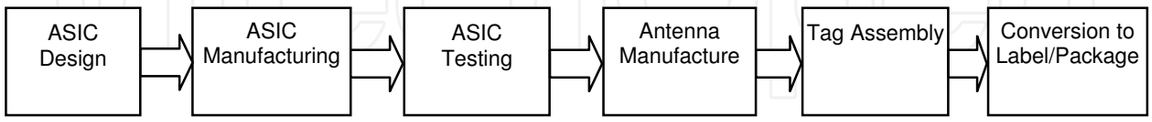

Fig. 2. RFID label/tag manufacturing process.

The design of silicon chips has been standardized for over 30 years and the cost of building a silicon fabrication plant is in the billions of US dollars (Hodges & Jackson, 1988; Baker et al, 1998). Since silicon chips are fabricated on a wafer-by-wafer basis there is a fixed cost per wafer (around US $1000). As the cost of the wafer is independent of the IC design, the cost of the RFID chip can be estimated based on the required silicon area for the RFID chip. Significant achievements have been made in reducing the size of the transistors allowing more transistors per wafer area (Natarajan, 2008). Decreasing the amount of transistors needed results in an even smaller silicon area, hence a lower RFID chip price. As a result, great efforts have been made by the Massachusetts Institute of Technology (MIT) to design a RFID ASIC with less than 8000 transistors. Although this will reduce the price of the silicon chip, its miniature size imposes limitations and further handling costs.

The cost of dividing the wafer, handling the die and placing them onto a label remains significant, even if the cost of the RFID chip were next-to-nothing. The cost of handling the die increases with the use of smaller than standard chips, simply because the electronics industry is not standardized for them. Hence, with highly-optimized low transistor count ASICs, implemented assembly processes and extremely large quantities (over 1 billion) of RFID chips sold per annum, a minimum cost of 5 cents is the reality for chipped RFID tags.

1.3 Chipless RFID tags

Given the inevitable high cost of silicon chip RFID tags (when compared to optical barcodes), efforts to design low cost RFID tags without the use of traditional silicon ASICs have emerged. These tags, and therefore systems, are known as **chipless** RFID systems. Most chipless RFID systems use the electromagnetic properties of materials and/or design various conductor layouts/shapes to achieve particular electromagnetic properties/behaviour. The main focus of this thesis will be on chipless RFID systems.

There have been some reported chipless RFID tag developments in recent years. However, most are still reported as prototypes and only a handful are considered to be commercially viable or available. The challenge for researchers when designing chipless RFID tags is how to perform data encoding without the presence of a chip. In response to this problem two general types of RFID tags can be identified: time domain reflectometry (TDR)-based and spectral (frequency) signature-based chipless RFID tags. Fig. 3 shows the classification of reported chipless RFID tags.

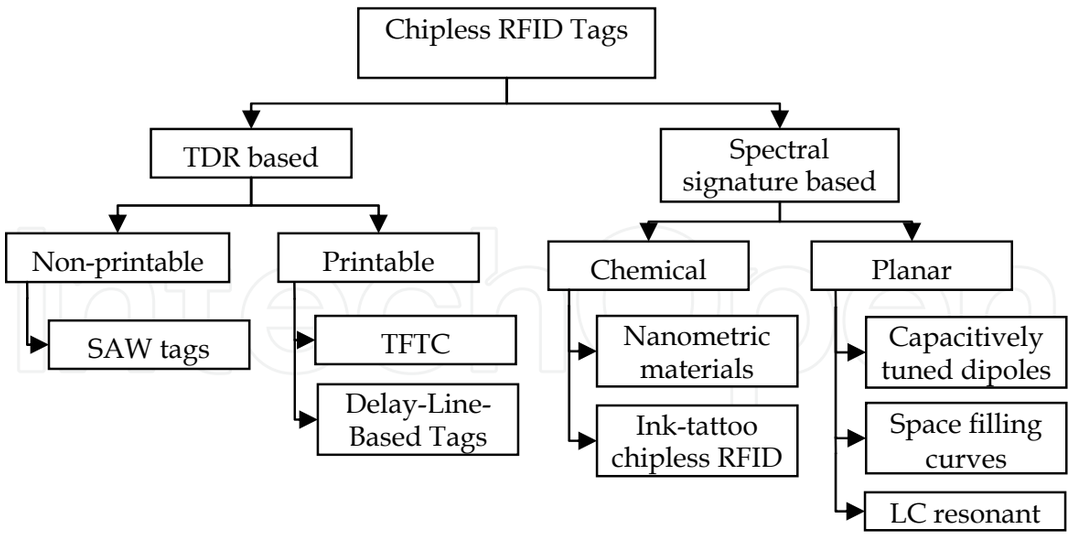

Fig. 3. Classification of chipless RFID tags.

TDR-based chipless RFID tags are interrogated by sending a signal from the reader in the form of a pulse and listening to the echoes of the pulse sent by the tag. A train of pulses is thereby created which can be used to encode data. Various RFID tags have been reported using TDR-based technology for data encoding. We can distinguish between non-printable and printable TDR-based tags.

An example of a **non-printable** TDR-based chipless RFID tag is the surface acoustic wave (SAW) tag developed by RFSAW Inc (Harma et al, 2006) which is also the commercially most successful. **SAW tags** are excited by a chirped Gaussian pulse sent by the reader centred around 2.45 GHz. The interrogation pulse is converted to a surface acoustic wave using an interdigital transducer (IDT). The surface acoustic wave propagates across the piezoelectric crystal and is reflected by a number of reflectors which create a train of pulses with phase shifts. The train of pulses is converted back to an EM wave using the IDT and detected at the reader end where the tag's ID is decoded (Hartmann, 2002).

Printable TDR-based chipless tags can be found either as Thin-Film-Transistor-Circuits (TFTC) or microstrip-based tags with discontinuities. **TFTC tags** are printed at high speed on low cost plastic film (Das & Harrop, 2006). TFTC tags offer advantages over active and passive chip-based tags due to their small size and low power consumption. They require more power than other chipless tags but offer more functionality. However low cost manufacturing processes for TFTC tags have not yet been developed. Another issue is the low electron mobility which limits the frequency of operation up to several MHz.

Delay-line-based chipless RFID tags operate by introducing a microstrip discontinuity after a section of delay-line as reported in (Shretha et al, 2007). The tag is excited by a short pulse (1ns) EM signal. The interrogation pulse is received by the tag and reflected at various points along the microstrip line creating multiple echoes of the interrogation pulse. The time delay between the echoes is determined by the length of the delay-line between the discontinuities. This type of tag is a replica of the SAW tag using microstrip technology which makes it printable. Although initial trials of and experiments on this chipless technology have been reported, only 4 bits of data have been successfully encoded, which shows the limited potential of this technology.

Spectral signature-based chipless tags encode data into the spectrum using resonant structures. Each data bit is usually associated with the presence or absence of a resonant peak at a predetermined frequency in the spectrum. So far, five types of spectral signature-based tags have been reported and all five are considered to be fully printable. We can distinguish two types of spectral signature tags based on the nature of the tag: chemical and planar circuit.

Chemical tags are designed from a deposition of resonating fibres or special electronic ink. Two companies from Israel use **nanometric materials** to design chipless tags. These tags consist of tiny particles of chemicals which exhibit varying degrees of magnetism and when electromagnetic waves impinge on them they resonate with distinct frequencies, which are picked up by the reader. They are very cheap and can easily be used inside banknotes and important documents for anti-counterfeiting and authentication. CrossID, an Israeli paper company, claims to have 70 distinct chemicals which would provide unique identification in the order of 2^{70} (over 10^{21}) when resonated and detected suitably (Glickstein, 2004). Tapemark also claims to have "nanometric" resonant fibres which are 5 microns in diameter and 1mm in length (Collins, 2004). These tags are potentially low cost and can work on low grade paper and plastic packaging material. Unfortunately, they only operate at frequencies up to a few KHz, although this gives them very good tolerances to metal and water.

Ink-tattoo chipless tags use electronic ink patterns embedded into or printed onto the surface of the object being tagged. Developed by Somark Innovations (Jones, 2007), the electronic ink is deposited in a unique barcode pattern which is different for every item. The system operates by interrogating the ink-tattoo tag by a high frequency microwave signal (>10 GHz) and is reflected by areas of the tattoo which have ink creating a unique pattern which can be detected by the reader. The reading range is claimed to be up to 1.2 m (4 feet). In the case of animal ID, the ink is placed in a one-time-use disposable cartridge. For non-animal applications the ink can be printed on plastic/paper or within the material. Based on the limited information available for this technology (which is still in the experimental phase) the author assumes that it is spectral signature based.

Planar circuit chipless RFID tags are designed using standard planar microstrip/co-planar waveguide/stripline resonant structures such as antennas, filters, and fractals. They are printed on thick, thin and flexible laminates and polymer substrates. **Capacitively tuned dipoles** were first reported by *Jalaly* (Jalaly & Robertson, 2005). The chipless tag consists of a number of dipole antennas which resonate at different frequencies. When the tag is interrogated by a frequency sweep signal the reader looks for magnitude dips in the spectrum as a result of the dipoles. Each dipole has a 1:1 correspondence to a data bit. Issues regarding this technology include: tag size (lower frequency longer dipole – half wavelength) and mutual coupling effects between dipole elements.

Space-filling curves used as spectral signature encoding RFID tags were first reported by *McVay* (McVay et al, 2006). The tags are designed as Peano and Hilbert curves with resonances centred around 900 MHz. The tags represent a frequency selective surface (FSS) which is manipulated with the use of space-filling curves (such as the Hilbert curve). The tag was successfully interrogated in an anechoic chamber. Only 3 bits of data have been reported to date. However, the tag requires significant layout modifications in order to encode data.

LC Resonant chipless tags comprise of a simple coil which is resonant at a particular frequency. These tags are considered 1-bit RFID tags. The operating principle is based on the magnetic coupling between the reader antenna and the LC resonant tag. The reader

constantly performs a frequency sweep searching for tags. Whenever the swept frequency corresponds to the tag's resonant frequency, the tag will start to oscillate, producing a voltage dip across the reader's antenna ports. The advantage of these tags is their price and simple structure (single resonant coil), but they are very restricted in operating range, information storage (1 bit), operating bandwidth and multiple-tag collision. These tags are mainly used for electronic article surveillance (EAS) in many supermarkets and retail stores (Tagsense, 2006).

2. Chipless RFID tag operating principle

In this book chapter we present a fully printable chipless RFID system based on multiresonators and cross-polarized ultra-wide band (UWB) monopole antennas. The tag's unique ID is encoded as the spectral signatures of the resonators. The main differences between the chipless RFID system presented here and others reported by McVay *et al* (McVay et al, 2006) and Jalaly *et al* (Jalaly & Robertson, 2005) are that we encode data in both amplitude and phase and the operation is not based on radar cross section (RCS) back-scattering. The chipless RFID system works on retransmission of the interrogation signal with the encoded unique spectral ID. The received and transmitted signals are cross-polarized in order to achieve good isolation between the two. Due to the robust design based on microwave engineering (multiresonators) and antenna technology (cross-polarized Tx/Rx antennas), we believe to have achieved less mutual coupling effects, greater number of possible bits and easier encoding than that reported by McVay *et al* and Jalaly *et al*.

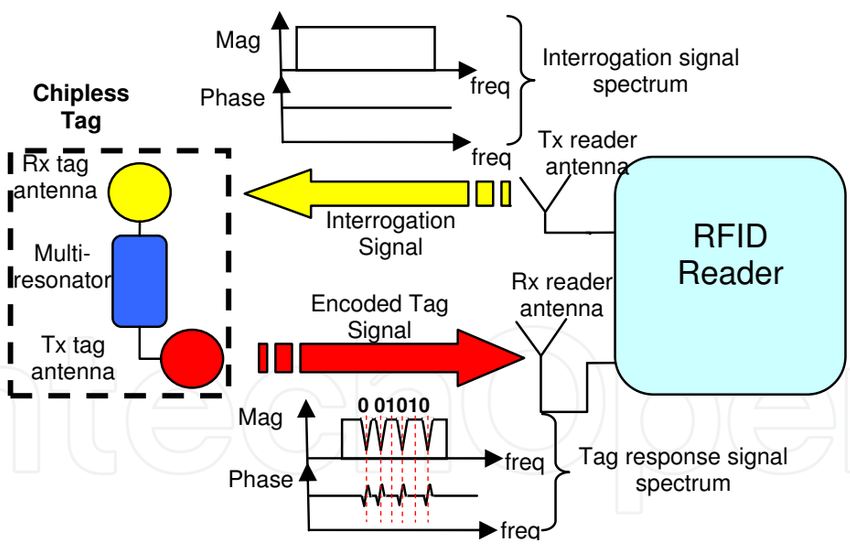

Fig. 4. Principal block diagram of chipless RFID system.

As the chipless RFID system uses spectral signatures for data encoding and is fully passive, the tags do not need any power supply in order to operate (Preradovic et al, 2009). The main application for this chipless RFID system is mainly short range (up to 40 cm) tagging of extremely low cost items. Hence, power limitation restrictions (transmitted EIRP maximum of -45 dBm outdoors and -55 dBm indoors), does not present a major concern for the presented system. The principal block diagram of the chipless RFID system is shown in Fig. 4. As can be seen in Fig. 4, the chipless tag encodes data in the frequency spectrum and thus

has a unique ID of spectral signatures. The spectral signature is obtained by interrogating the tag by a continuous wave (CW) multi-frequency signal of uniform amplitude and phase. The tag then receives the interrogation signal and encodes the data into the frequency spectrum in both magnitude and phase. The encoded signal is then retransmitted back to the reader. This allows the reader to use two criteria for data decoding – amplitude and phase.

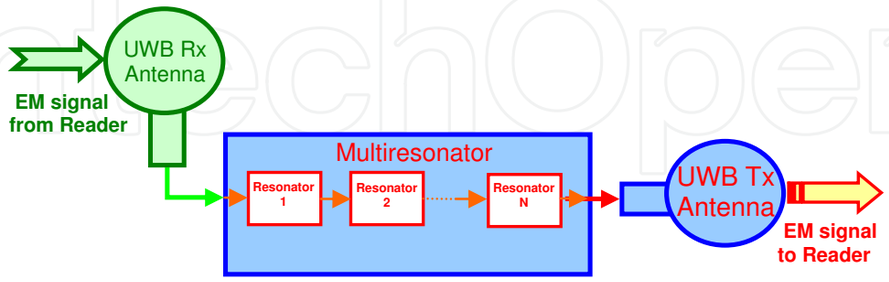

Fig. 5. Block diagram of chipless RFID tag.

The chipless RFID tag consists of UWB antennas and a multiresonating circuit operating in the UWB frequency spectrum as shown in Fig. 5. The UWB antennas are used to receive the interrogation signal sent from the reader and transmit the signal back to the reader after performing spectral signal modulation by the multiresonator. The multiresonator is a combination of multiple filtering sections which are used to modulate the spectrum of the interrogation signal sent by the reader. Modulation is performed in both magnitude and phase of the spectrum.

The chipless RFID reader is an electronic device which can detect the ID of the chipless tag when it is within the reader's interrogation zone. The block diagram of the chipless RFID reader is shown in Fig. 6. The RFID reader has transmitting and receiving antennas to send the interrogation signal to the chipless tags and receive the encoded signal from the chipless tags. The RFID reader transmitter comprises a voltage controlled oscillator (VCO), low noise amplifier (LNA) and power amplifier (PA). Tuning of the VCO's output frequency is done by the microcontroller through the digital-to-analog (ADC) converter. The reader transmitter generates the interrogation signal which is sent to the chipless tag. The chipless tranponder encodes its spectral signature into the reader's interrogation signal and sends the signal back to the reader. The signal flow diagram of the chipless RFID system is shown in Fig. 7.

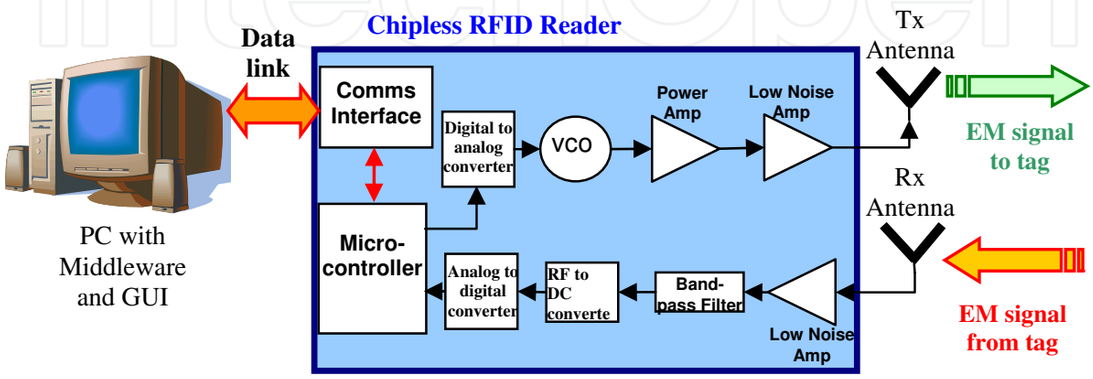

Fig. 6. Block diagram of proposed chipless RFID reader.

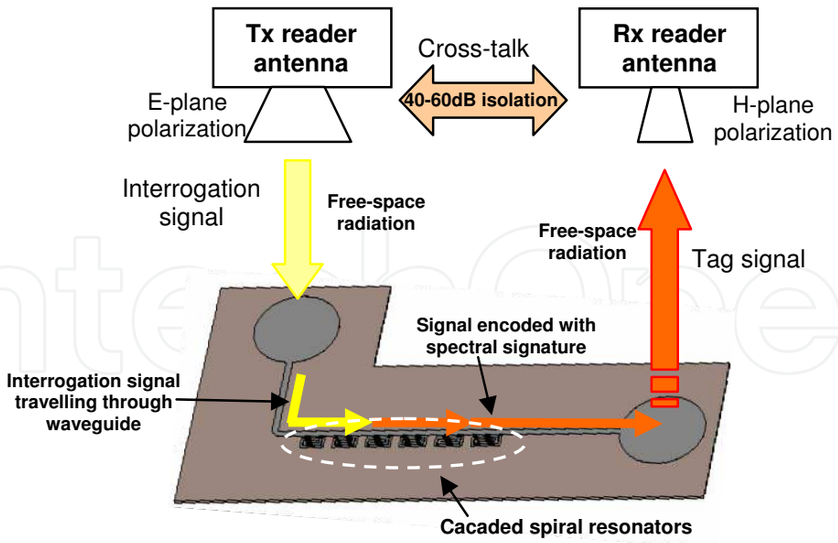

Fig. 7. Chipless RFID system signal flow diagram.

The chipless tag encodes data in the frequency spectrum thus encoding the spectrum with its unique spectral signature. The spectral signature is obtained by the RFID reader by interrogating the tag by a multi-frequency signal. The tag encodes its spectral signature into the interrogation signal spectrum using a multiresonating circuit which is a multi-stop band filter. The multiresonator is a set of cascaded spiral resonators designed to resonate at particular frequencies and create stop bands. The stop band resonances introduce magnitude attenuation and phase jumps to the transmitted interrogation signal at their resonant frequencies which are detected as abrupt amplitude attenuations and phase jumps by the RFID reader. In order to provide isolation between the transmitting and receiving signal, the reader and tag antennas are cross-polarized. As a result, cross-talk between the transmitting and receiving antennas is minimized at the cost of introducing restrictions in tag positioning and orientation.

The chipless RFID system is designed for a short range conveyor belt system where the tagged items are tracked moving through the interrogation zone of a fixed reader antenna system as shown in Fig. 8.

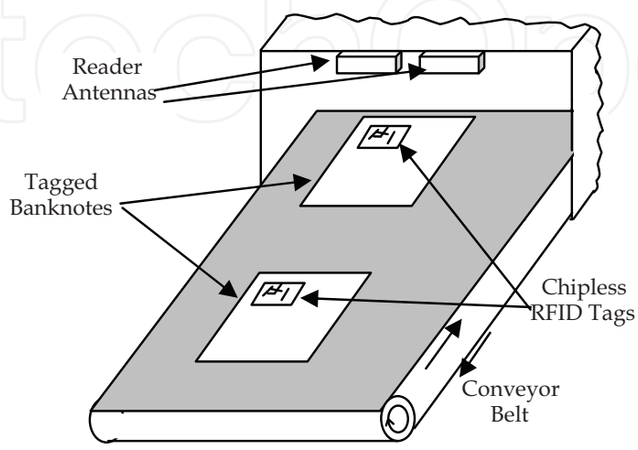

Fig. 8. Potential conveyor belt application for chipless RFID system.

3. Chipless RFID tag development

In this section the chipless tag development is presened. The tag design steps are shown in Fig. 9. The tag design was begun by designing the tag monopole antennas and achieving the necessary return loss bandwidth and radiation pattern. Following the tag antenna design, design and optimization of the spiral resonators (multiresonating circuit) were carried out. When the tag antenna and multiresonating circuit were optimized they are integrated to form a complete chipless RFID tag which were then tested in a wireless experimental setup inside an anechoic chamber (for theoretical verification) and in a laboratory (for investigations of robustness). In the following sections, the design of the tag antenna, multiresonator and integrated tag are presented

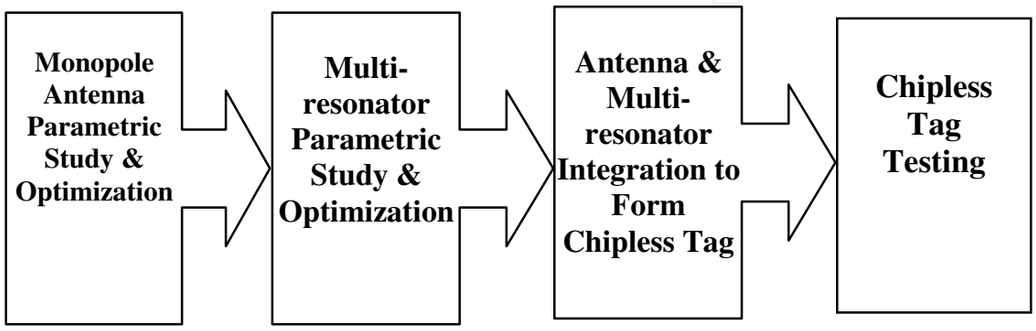

Fig. 9. Chipless Tag design process.

3.1 Chipless tag antenna - UWB monopole

Circular UWB monopole antennas have a simple layout and exhibit extremely large bandwidth and a figure-of-eight radiation pattern (Chen et al, 2007; Alipour & Hassani, 2008; Wu et al, 2008). UWB dipole antennas have been reported by researchers with similar radiation properties and bandwidth as those found using UWB monopoles (Quintero & Skrivervik, 2008; Mudroch et al, 2009; Whyte et al, 2008). Both types of antennas are fully printable and initially appear suitable for deployment as the chipless RFID tag antenna. The main disadvantage of UWB dipoles when compared to UWB monopoles is that they require an impedance matching circuit and/or balun which can increase the size and complexity of design of the tag. As UWB monopole antennas need no impedance matching circuit or balun for their successful operation, they are a preferred solution for the chipless RFID tag antenna. The UWB characteristic of the monopole antenna is attributed to the overlapping of the antenna modes (resonances) which are closely distributed over the spectrum (Angelopoulos et al, 2006). The operational principle of the UWB disc monopole is shown in Fig. 10. The use of the higher order modes influences the monopole's radiation pattern in the E-plane which becomes distorted from a figure-of-eight radiation pattern in the fundamental mode. At the antenna's fundamental mode of operation the wavelength of the transmitting/receiving signal is greater than the antenna's dimensions and because the antenna operates in an oscillating mode a standing wave is formed. As the frequency of the signal (and therefore operation) increases, the antenna starts operating in a hybrid mode of standing and travelling waves. At higher frequencies the travelling waves are dominant since the wavelengths at these frequencies are smaller than the antenna structure. Therefore, due to the hybrid modes of antenna operation it is possible to create an extremely wide-

band operating antenna at the expense of radiation pattern distortion at higher operating modes. These distortions are due to the surface current distribution in higher order modes. The H plane radiation pattern remains constant throughout the operating band. This is due to the symmetry of the antenna's configuration along its axis of rotation.

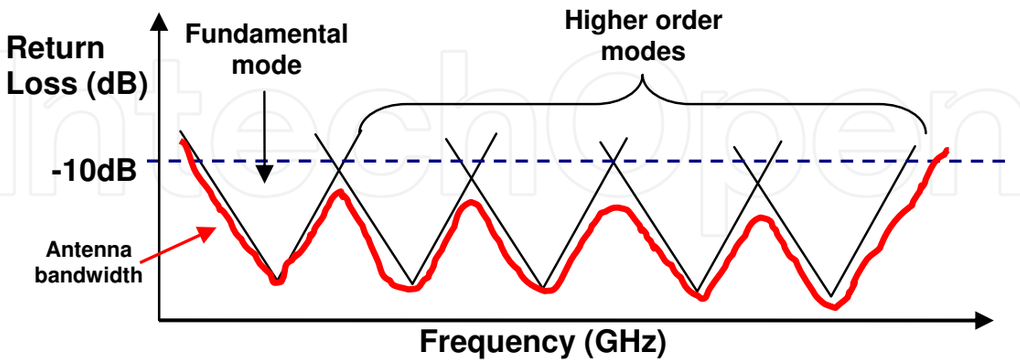

Fig. 10. UWB monopole operational principle.

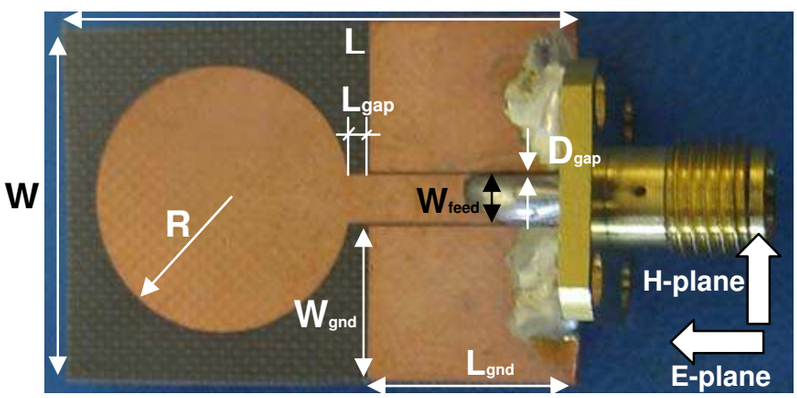

Fig. 11. Photograph of CPW fed UWB monopole (L = 27 mm, W = 18.8 mm, Lgnd = 12 mm, Wgnd = 8mm, Dgap = 0.15 mm, Lgap = 2 mm, Wfeed = 2.5 mm and R =7 mm, substrate Taconic TF-290 ε_r = 2.9, h = 0.09 mm, tanδ = 0.0028).

The CPW disc monopole antenna is a single layer-metallic structure comprised of a copper disc with radius *R* and a 50Ω CPW printed on the same side of the dielectric substrate Taconic TF-290 (εr=2.9, h=90μm, tanδ=0.0028). The manufactured CPW monopole antenna with design parameters is shown in Fig. 11.

3.2 Chipless tag multiresonator

In this section the design of the chipless tag multiresonator is presented. The chipless tag encodes data by using spectral signature encoding. Each tag has a different spectral signature by filtering out a predefined set of frequencies. The multiresonator circuit comprises a set of cascaded spiral resonators which resonate at different frequencies.

Coplanar waveguide (CPW) technology was used for designing high Q spiral resonators. The CPW was first proposed by C. P. Wen in 1969 (Wen, 1969). Wen proposed the novel waveguide as a dielectric substrate coated with a single layer of copper. It consists of a conductor centre strip with conductive ground plane sheets on both sides of the strip. The

impedance of the strip is determined by the width of the strip, the gap, the permittivity and thickness of the dielectric. In practice this means that we can have multiple widths of the CPW strip on the same dielectric which would have, for example, a 50 ohm impedance at the cost of modification of the gap between the strip and ground planes. This property of CPW makes it a very flexible transmission line technology. CPW technology uses spiral shapes etched out in the stripline to create stop bands. The layout of a spiral resonator designed on 90 µm thin Taconic TF-290 laminate is shown in Fig. 12.

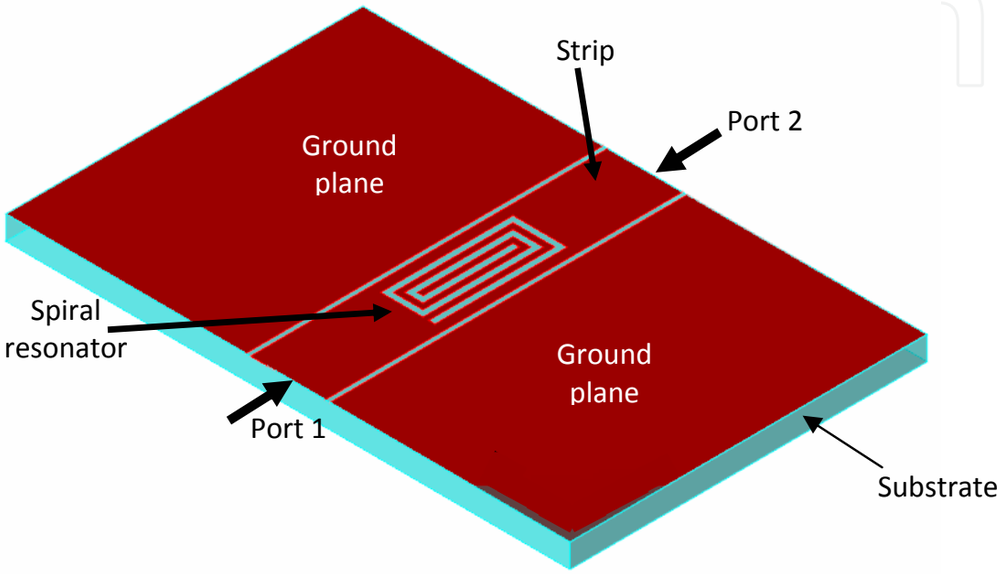

Fig. 12. Layout of spiral resonator etched out in a CPW strip line.

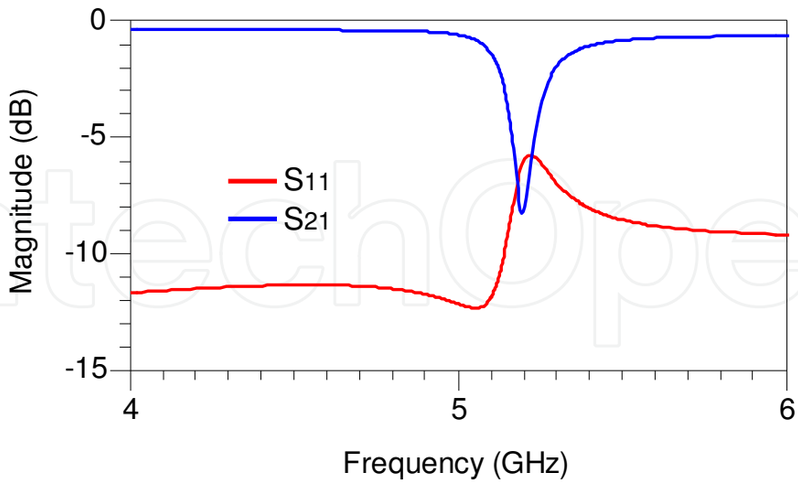

Fig. 13. Simulated frequency response of spiral resonator etched out in a CPW strip line on TF-290 (εr = 2.9, h = 90 µm, tanδ = 0.0028).

The CPW the ground plane and the spiral resonator are on the same plane (top layer). The strip line is separated from the continuous metallic ground planes by a gap. At its resonant frequency, the spiral resonator creates a stop band as can be seen in Fig. 13. The 2-port s-

parameters of the CPW spiral resonator were obtained from ADS Momentum 2008. The CPW spiral resonator was designed on Taconic TF-290 (εr = 2.9, h = 90 μm , tanδ = 0.0028). Each spiral resonator introduces a different stop-band resonance. By varying the dimensions of the spiral resonator we can vary the resonance. Fig. 14 shows the variation of the spiral's resonant frequency and attenuation with the spiral's resonator length L_{spiral} as obtained from ADS 2008 Momentum simulation.

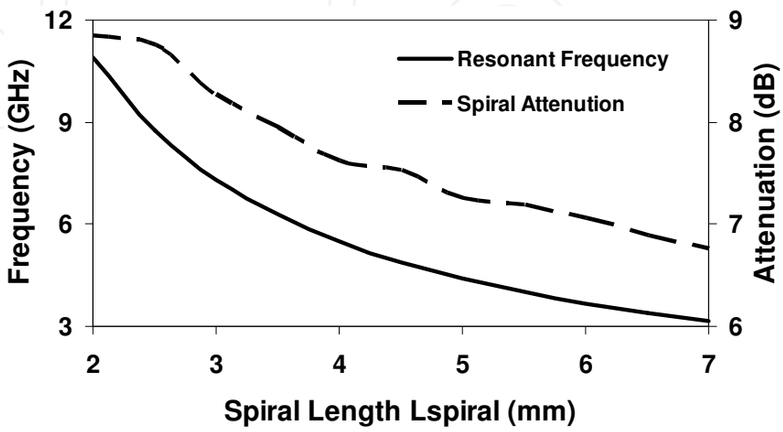

Fig. 14. CPW spiral resonant frequency and attenuation vs spiral length L_{spiral}.

The advantages of the CPW spiral resonator in comparison to the microstrip spiral resonator are higher attenuation at resonant frequency and the single sided layout. The disadvantages are in terms of compact layout, since CPW spiral resonators can be cascaded only by placing them in series. Fig. 15 shows a photograph of the fabricated 3-bit multiresonator on TF-290 substrate. The 3-bit multiresonator consists of 3 spiral resonators cascaded within a 50 ohm CPW strip line. The spirals are etched in the CPW strip line. The CPW multiresonator provides 3 distinguishable resonances between 2 and 2.5 GHz. Each resonance is separated by approximately 200 MHz from each other. In order to design the spirals at different frequencies, the length of each spiral has been varied so that the spiral's resonant frequency is tuned.

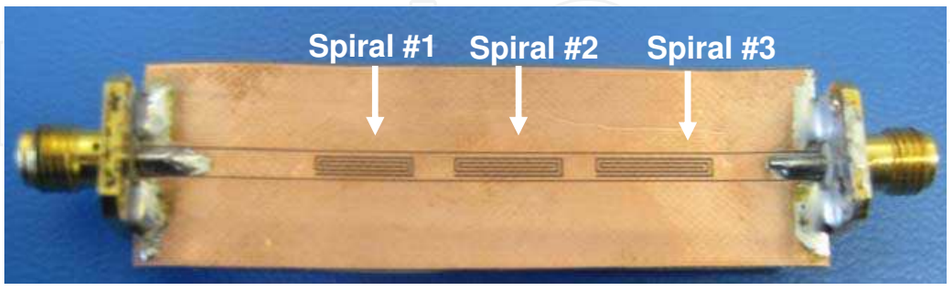

Fig. 15. Photograph of manufactured CPW 3-bit multiresonator on 90 μm Taconic TF-290 substrate.

Fig. 16 shows the simulated frequency response in both magnitude and phase of the 3-bit multiresonator. From Fig. 16 it is clear that at the resonant frequencies of each spiral of the multiresonator there is a magnitude null and phase jump in the magnitude and phase of the spectrum of the CPW multiresonator. These distinct nulls and jumps in magnitude and

phase respectively are interpreted as logic "0" while their absences at the resonant frequencies are interpreted as logic "1".

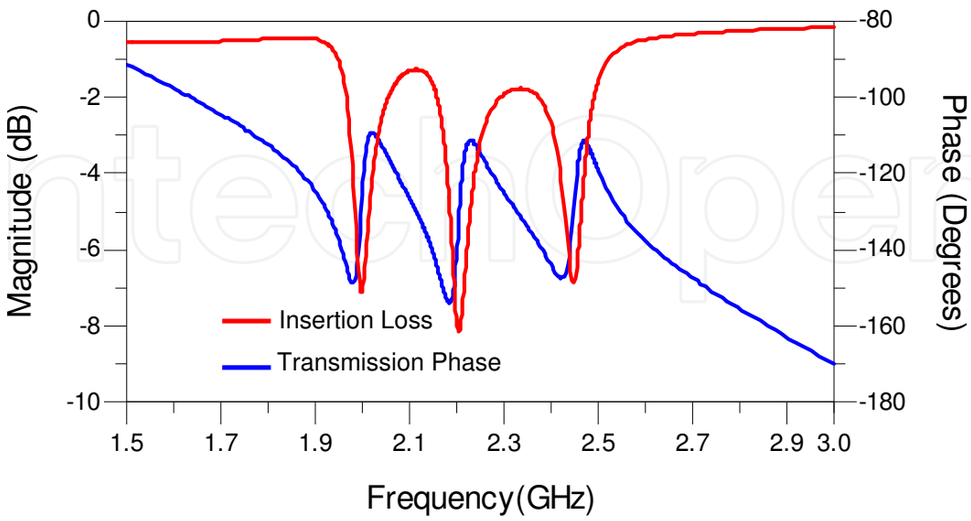

Fig. 16. Measured insertion loss and transmission phase of CPW 3-bit multiresonator.

3.3 Encoding data using spiral shorting

It is necessary to encode data into the tag in order for the tag to have a unique ID. The short ing of the turns of the spiral as shown in Figs 17 creates shifting of the resonance frequency of the spiral up where it will be of no significance. The shift of the resonant frequency with the shorting of the turns is shown in Fig. 18. The advantage of shorting turns over to removing the entire spiral from the layout is that it enables future printing techniques to preserve the layout with all of the spirals shorted and when encoding data the shorting can be removed via a laser or other etching technique. The frequency signatures of tags with different IDs are shown in Figs 19 and 20.

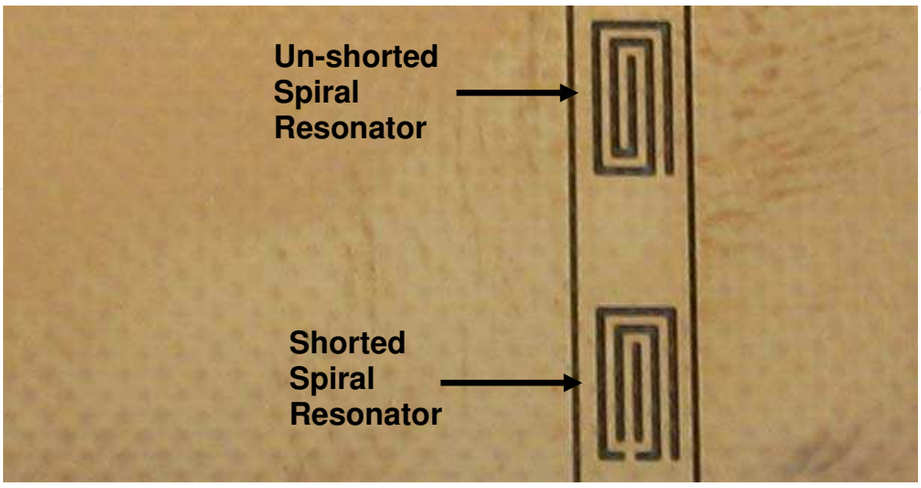

Fig. 17. Photograph of removing spiral resonances via spiral shorting for CPW multiresonator.

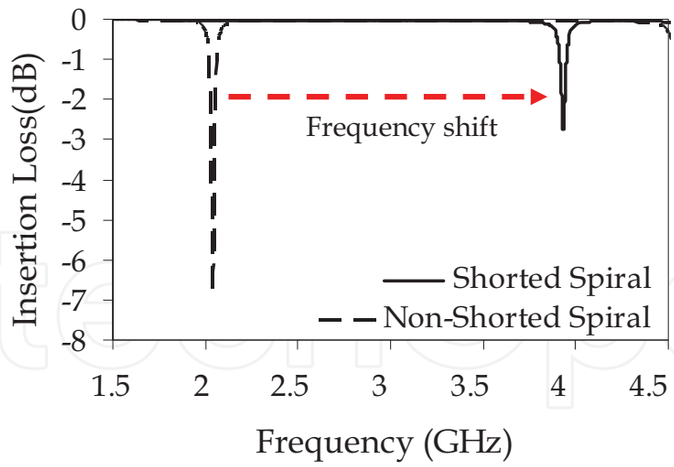

Fig. 18. Frequency shift of resonant frequency with short-circuited spiral.

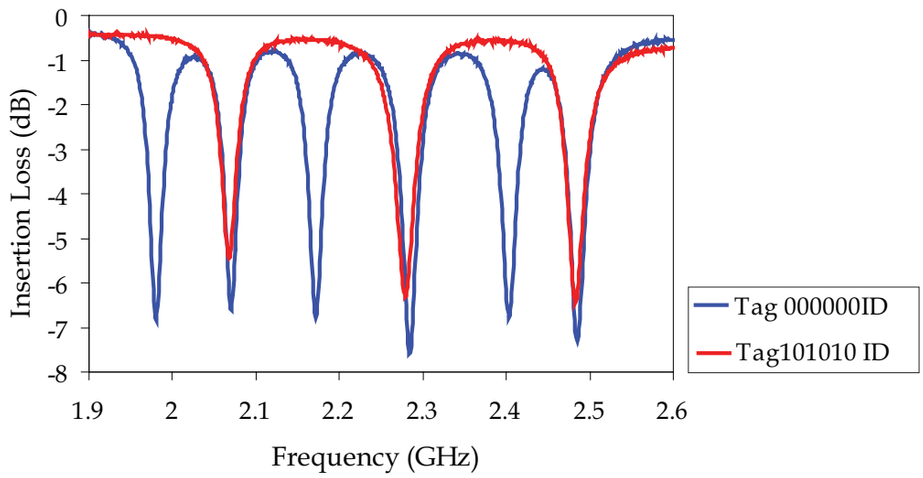

Fig. 19. Measured insertion losses of chipless tags with different spectral signatures.

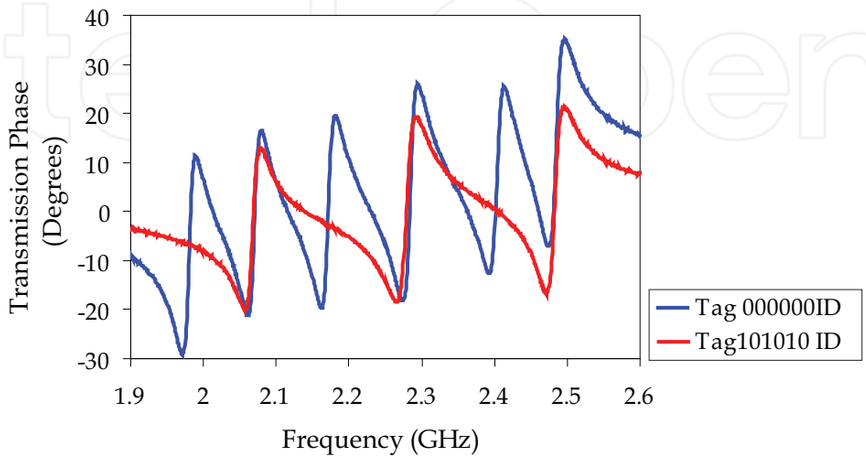

Fig. 20. Measured transmission phases of chipless tags with different spectral signatures.

3.4 Chipless RFID tag

The flexible chipless tag was designed on laminate Taconic TF-290 (εr = 2.9, h = 90 µm, tanδ = 0.0028) using ADS Momentum 2008. For this purpose, the antenna and multiresonators were designed individually. The layout of the chipless RFID tag with design parameters printed on flexible TF-290 laminates is shown in Fig. 21. The tag was designed on CPW, making it single-sided.

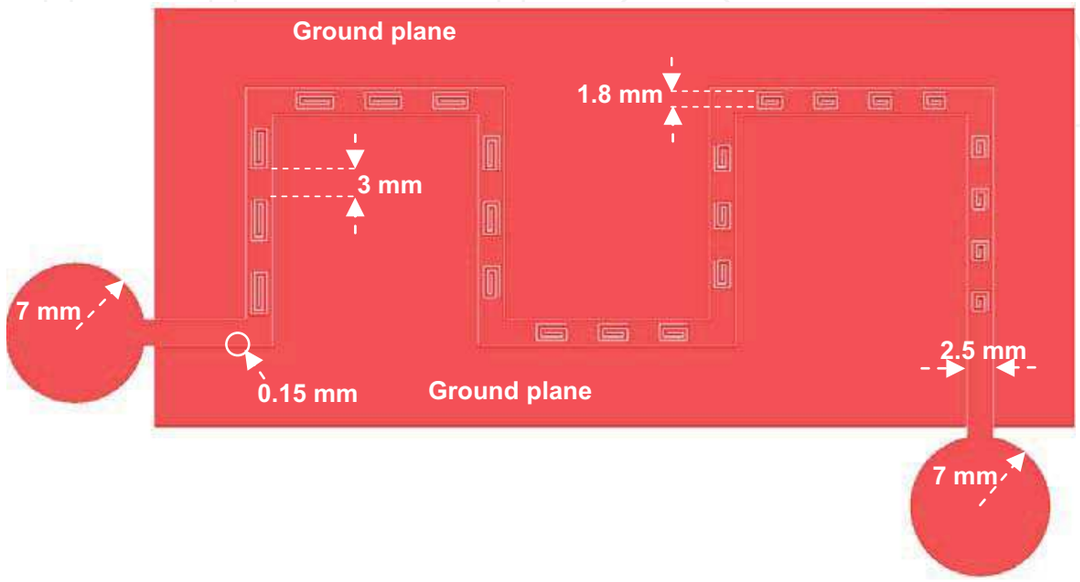

Fig. 21. Layout of integrated flexible CPW 23-bit chipless tag with design parameters on Taconic TF-290 laminate (εr = 2.9, h = 0.09 mm, tanδ = 0.0028).

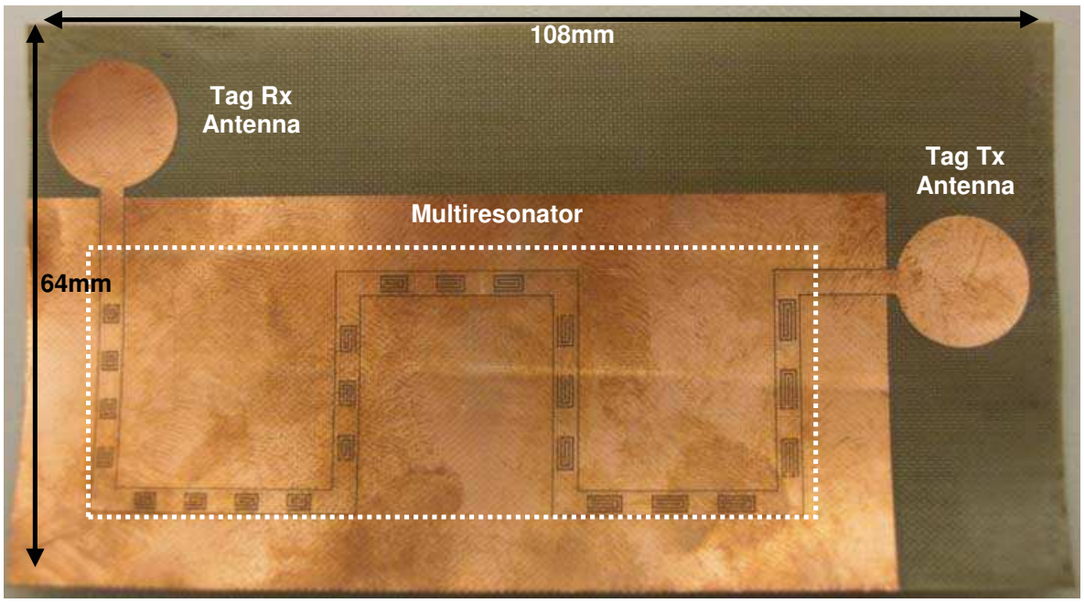

Fig. 22. Photograph of 23-bit chipless RFID tag on Taconic TF-290 (εr = 2.9, h = 90 µm, tanδ = 0.0028).

A photograph of the tag is shown in Fig. 22. The tag encodes 23 bits of data between 5 and 10.7 GHz. The chipless tag is comprised of a vertically- polarized UWB disc-loaded monopole receiving tag antenna, a multiresonating circuit and a horizontally-polarized UWB transmitting tag antenna designed using CPW technology. The chipless tag is designed to fit the Australian banknote and its dimensions are 108mm by 64mm. The spirals were etched out with the spiral trace and separation between spiral traces being 0.2 mm. The 50 ohm CPW strip line was designed to be 2.5 mm with the gap separation from the ground plane being 0.15 mm. The spirals were etched in the strip line with a 3 mm separation between adjacent cascaded spirals.

4. Results

4.1 UWB monopole

The measured antenna return loss vs frequency is shown in Fig. 23. The antenna yields UWB operation with greater than 10 dB return loss from 5 to 11 GHz.

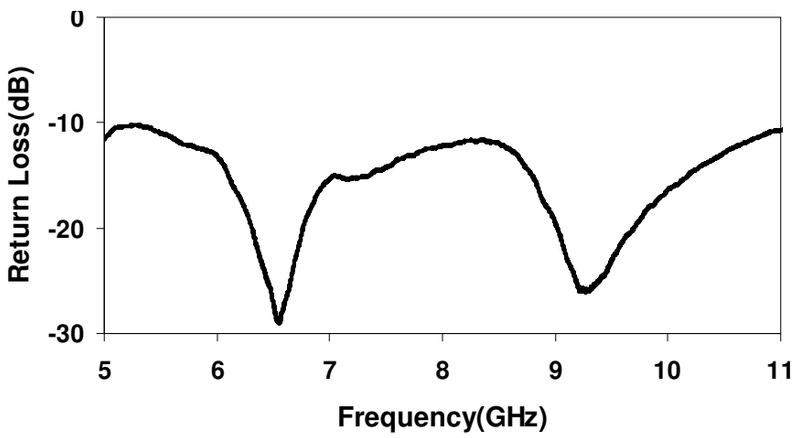

Fig. 23. Measured return loss of chipless RFID tag UWB monopole antenna.

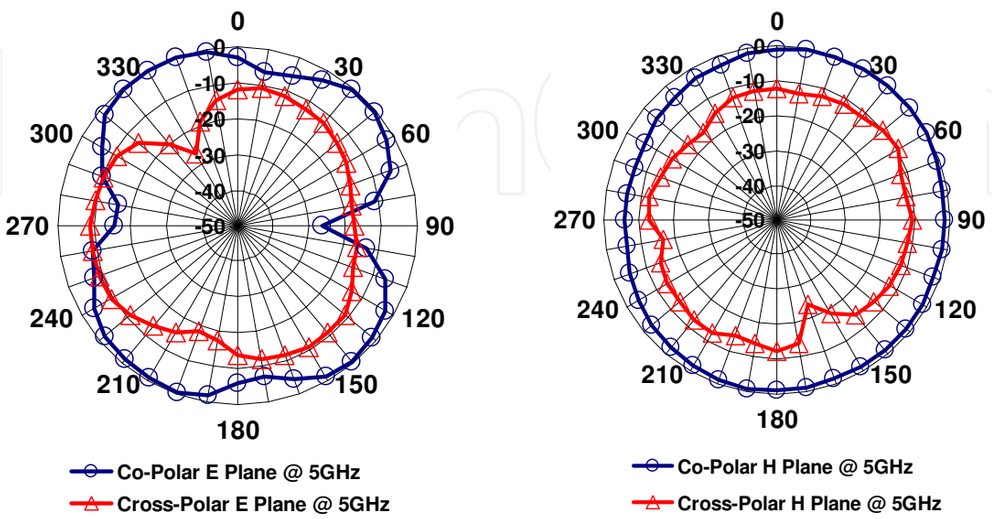

Fig. 24. Measured co-polar and cross-polar radiation patterns of UWB monopole at 5 GHz.

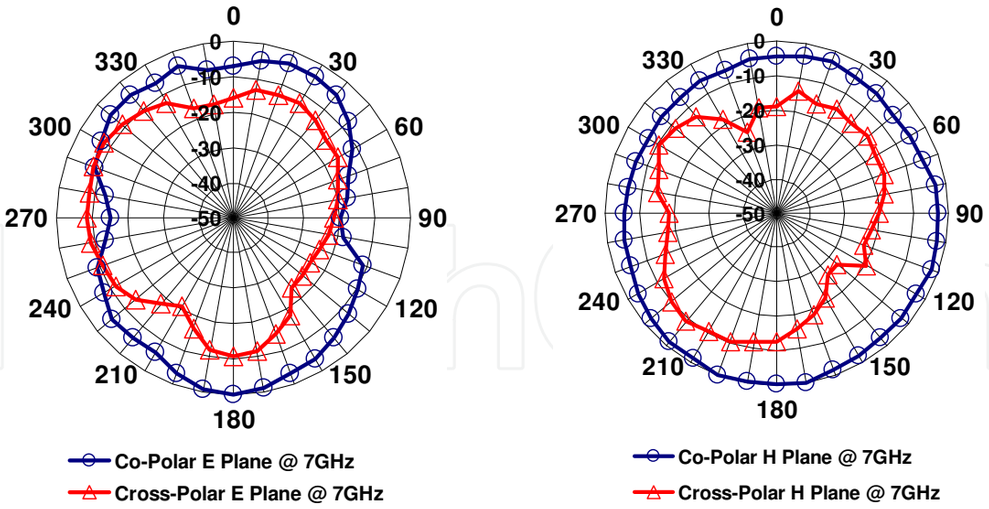

Fig. 25. Measured co-polar and cross-polar radiation patterns of UWB monopole at 7 GHz.

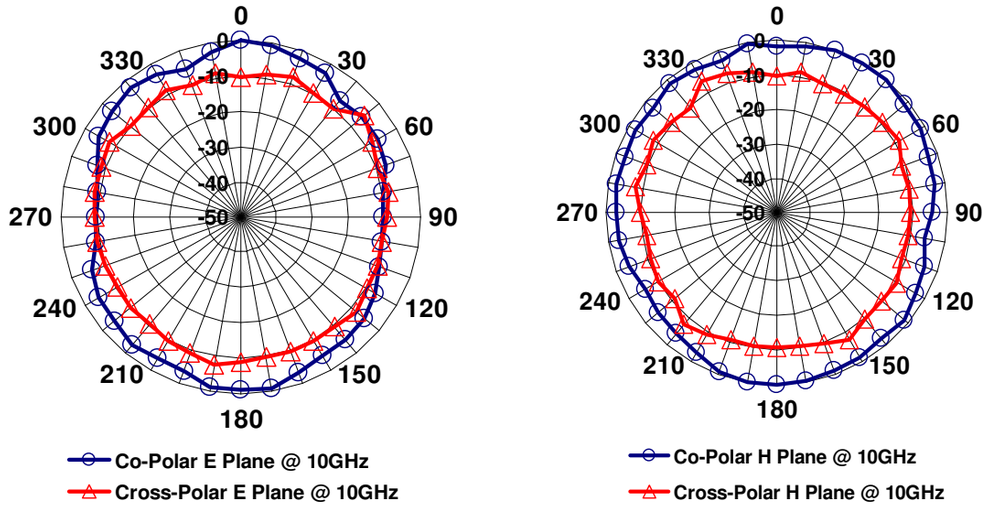

Fig. 26. Measured co-polar and cross-polar radiation patterns of UWB monopole at 10 GHz.

Fig. 23 shows multiple operating modes of the UWB monopole antenna. In order to achieve extremely large bandwidth, UWB monopole antennas rely on the overlapping of their modes. Hence, changes in radiation patterns are expected with frequencies outside the monopole's fundamental mode of operation of around 4.2 GHz. The antenna co-polar and cross-polar radiation patterns from 5-10 GHz in both E and H planes (as shown in Fig. 11) are presented in Figs 24, 25 and 26.

The tag antennas show good cross-polar component suppression (at least in the order of 10 dB average) which is essential for robust readings and isolation between the interrogation signal and encoded signal.

4.2 Multiresonator

The CPW-based UWB 23-bit chipless RFID tag encodes 23 bits of data from 5 to 10.7 GHz. The tag is printed on thin flexible laminate Taconic TF-290. The 23 bits of data are encoded

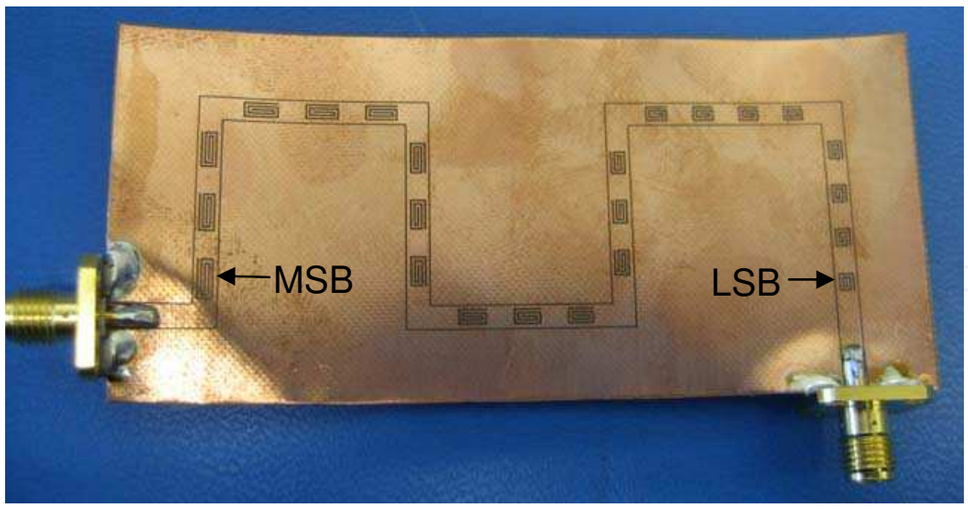

Fig. 27. Photograph of the 23 spiral multiresonating circuit on TF-290.

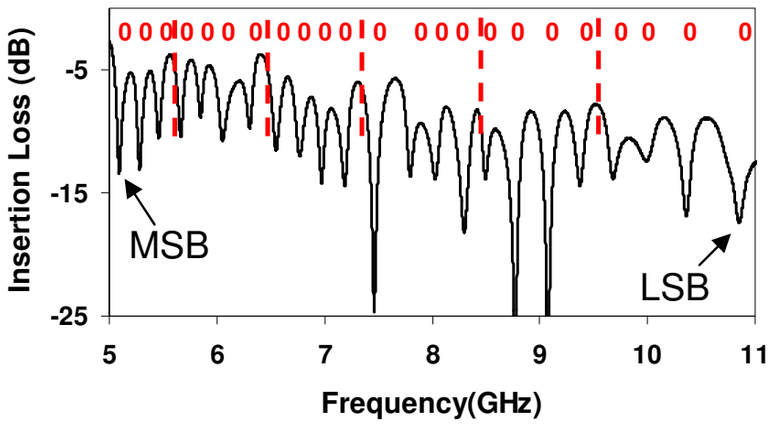

Fig. 28. Measured tag insertion loss of 23 bit tag ID "0x000000".

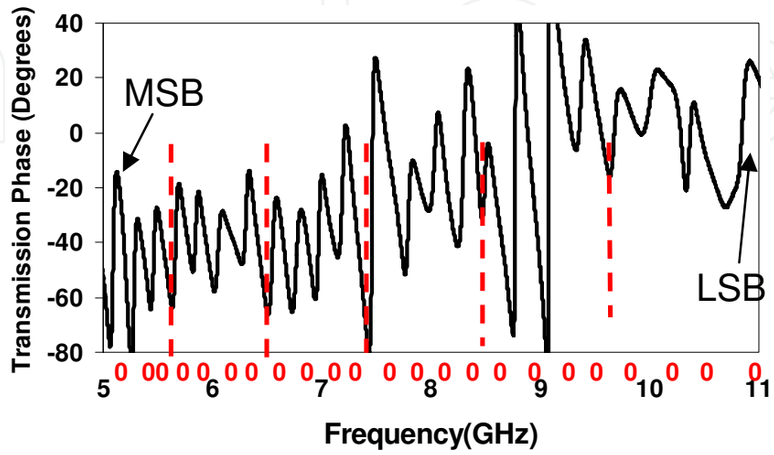

Fig. 29. Measured tag transmission phase of 23 bit tag ID "0x000000".

using a 23 spiral multiresonating circuit shown in Fig. 27. The measured spectral signatures in both insertion loss vs frequency and transmission phase vs frequency of the 23-bit tag are shown in Figs 28 and 29 respectively. From Figs 28 and 29 it is clear that the 23 logic '0' bits are detected in the magnitude as magnitude nulls (or dips) while their phase signature is represented by 23 phase jumps. These measurements confirm the successful operation of the multiresonator.

4.3 Field trials

The experimental setup in the anechoic chamber consists of the chipless tag, the vector network analyzer (VNA) PNA E8361A as the reader electronics and horn antennas as the reader antennas. Horn antennas were used to increase the reading range of the tag since they have high gain (~11 dBi). The experiment was conducted in the Monash University Anechoic Chamber in order to validate the successful encoding of the tag and its detection at the reader end using the network analyzer. The chipless tag and the reader antennas were mounted on plastic stands and placed into the anechoic chamber. A block diagram of the experimental setup is shown in Fig. 30.

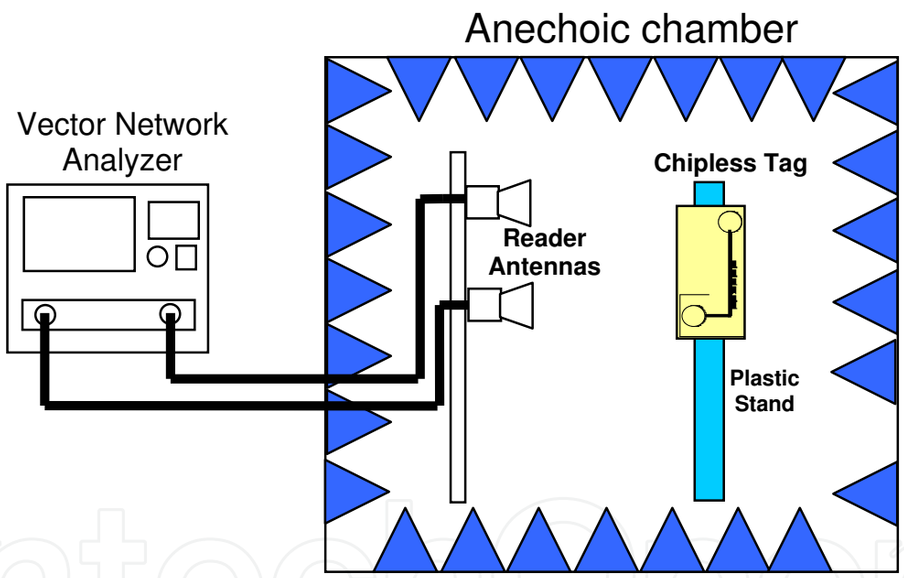

Fig. 30. Block diagram of the anechoic chamber setup.

As the horn antennas covered the frequency range from 7 - 12 GHz, the tag was interrogated starting from 7 GHz. This resulted in reading 13 bits of the entire 23-bit data encoded by the tag. However, this was sufficient to prove the successful operation of the tag and provide a read range estimation using horn antennas. A photograph of the experimental setup is shown in Fig. 31.

The use of horn antennas as reader antennas in this experimental setup greatly increased the reading range of the tag. We attribute this to the greater isolation of the cross-polarized reader antennas, and their higher directivity and higher gain than those of the log periodic arrays (presented in Chapter 4). The cross-polar reader antennas are shown in Fig. 32. As can be seen from Fig. 33, the isolation between the reader antennas is well above 65 dB.

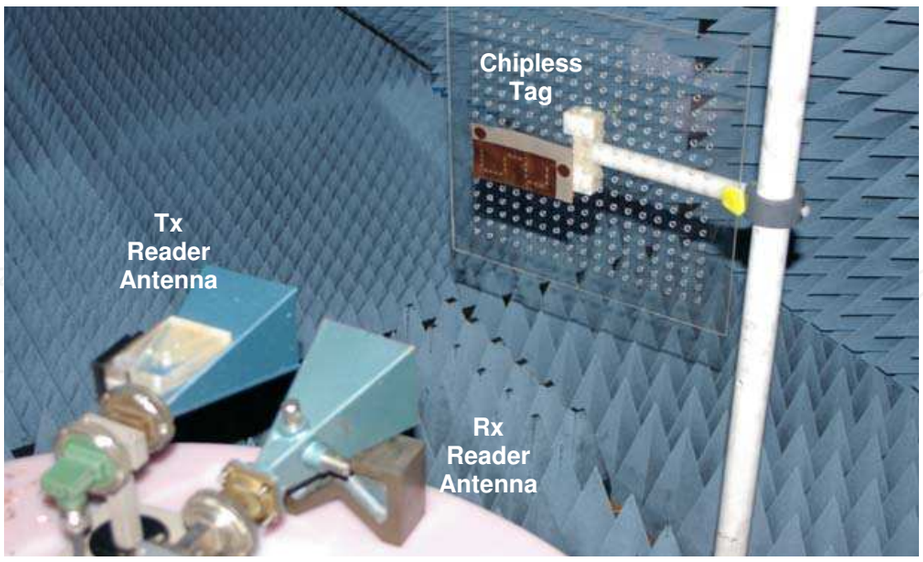

Fig. 31. Photograph of the experimental setup in the anechoic chamber of UWB RFID system.

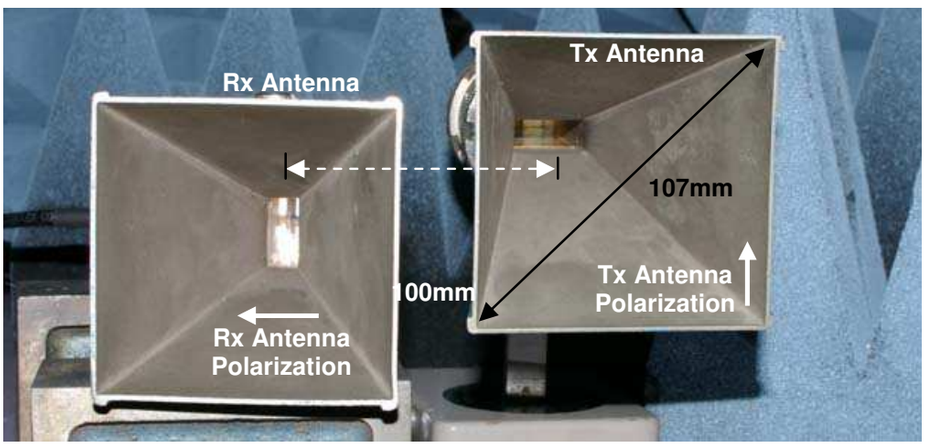

Fig. 32. Photograph of cross-polarized horn antennas used at reader end with 10cm separation.

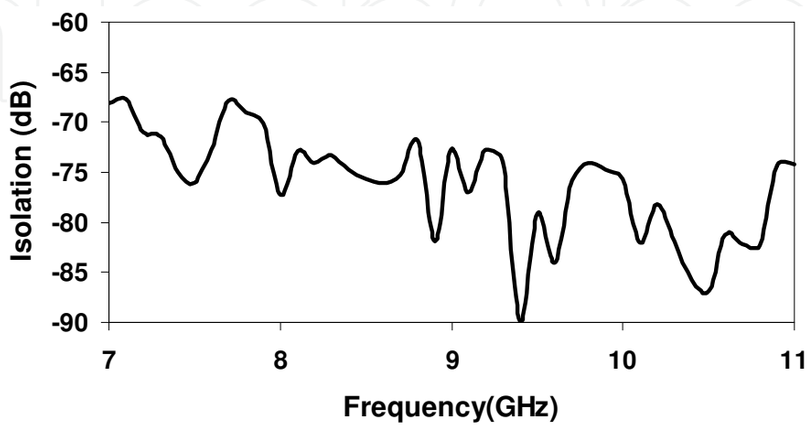

Fig. 33. Measured isolation between cross-polarized reader horn antennas.

We encoded the tag with ID '0x000000'and placed it from 5 cm to 70 cm (in steps of 5 cm) away from the horn reader antennas as shown in Fig. 31. The PNA was calibrated with the output power at the ports being -28 dBm. Both amplitude and phase data were retrieved when interrogating the tag. The chipless RFID tag was detected using a reference tag "0x111111" which carried no resonances. Hence, when the two results were compared the encoded resonances from tag ID '0x000000' were successfully detected. The normalized magnitude and phase of tag ID"0x000000" at 10 cm are presented in Figs 34 and 35 respectively. The measured results vs distance of tag from reader antennas are shown in Fig. 36.

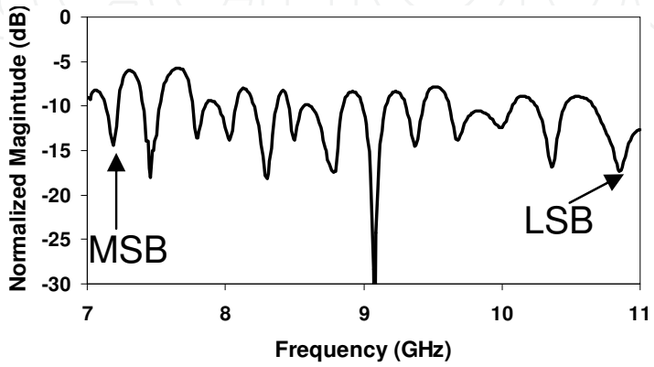

Fig. 34. Normalized magnitude variation vs frequency of chipless RFID tag with ID"0000000000000" from 7 – 10.7 GHz.

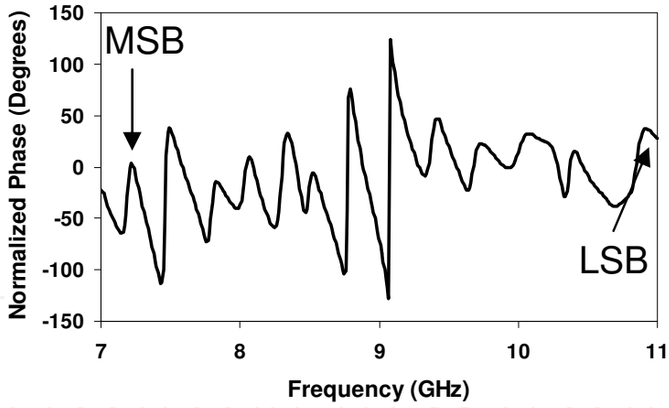

Fig. 35. Normalized phase variation vs frequency of chipless RFID tag with ID"0000000000000" from 7 – 10.7 GHz.

From Fig. 36 it is clear that in the anechoic chamber the tag can be detected further away (up to 70 cm) when using phase data detection than when using amplitude data detection. This is attributed to the greater robustness of phase when compared to amplitude. The successful interrogation of the tag in both amplitude and phase was conducted up to 50 cm. This result shows an improvement in the reading range detection of 300% in amplitude data and 75% in phase data (up to 70 cm) compared with the results reported in the previous section. The increased reading range in amplitude was greatly influenced by the increase of the cross-polar isolation of the tag antennas, increased isolation between the reader horn antennas and higher gain of the reader antennas (~11dBi over the entire band).

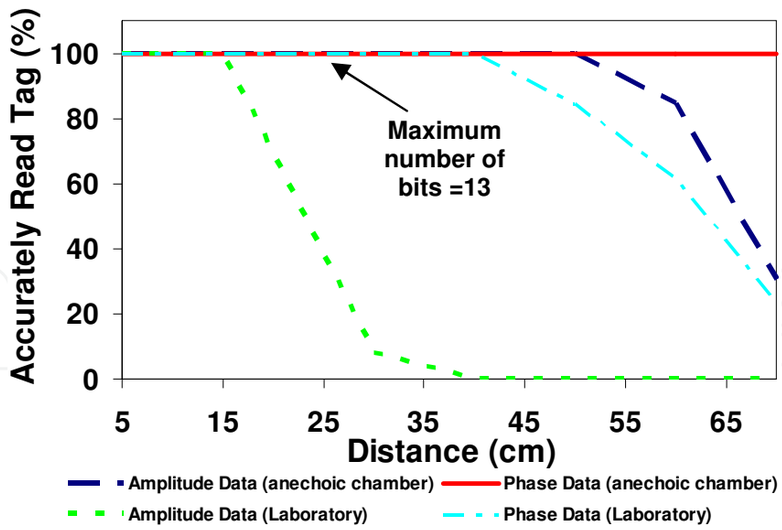

Fig. 36. Number of successfully detected bits vs distance of tag from reader antennas from 7 – 10.7 GHz (maximum of 13 detectible bits).

The chipless tag was placed in a laboratory setup (outside the anechoic chamber Fig. 37) in order to measure the detection range of this particular setup when exposed to environmental influences.

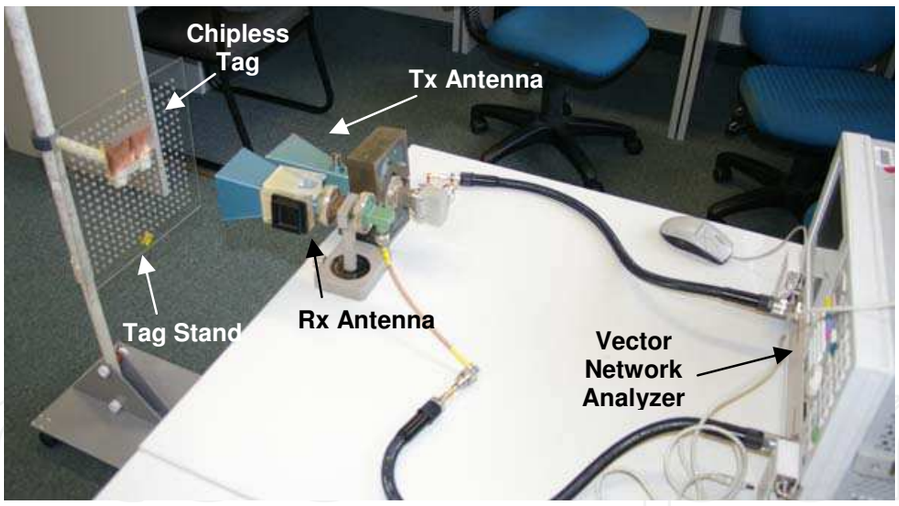

Fig. 37. Photograph of the experimental setup in the laboratory.

Fig. 36 shows that the tag was read accurately in both amplitude and phase up to 15 cm when placed in a laboratory as shown in Fig. 37. The phase data were detectable at greater reading ranges (up to 35 cm) than the amplitude data due to robustness of the phase data. Fig 36 clearly shows that the reading range dropped by 50% outside the anechoic chamber due to interference from the environment. However, it should be mentioned that the detection procedure was a simple comparison of tag data with no resonances and tag data with all resonances. The reading range could be improved by using signal processing techniques (such as matched filtering) to isolate the tag signal from the noise and interference and thus increase the reading range (Hartmann et al, 2004).

5. Conclusion

In this chapter we have presented the development and testing of a chipless RFID tag based on multiresonators. The development and successful testing of the chipless RFID tag meets the demand for a fully-printable ultra-low cost tag used for tagging items on conveyor belts. The salient feature of the novel chipless RFID tag is its fully-printable single-layered design in a compact and low cost format. It has significant amount of data encoding capability (up to 23 bits were designed).

Prior to the design and development of the chipless RFID tag a comprehensive literature review of RFID tags was conducted. The goal of the literature review was to identify the niche areas of design and development in RFID in which novel research could be carried out. The comprehensive literature review of chipless RFID tags revealed that chipless tags which are fully printable, multi-bit with ease of data encoding were not currently available. Some work had been carried out on capacitively tuned dipoles and fractal Hilbert curve-based tags but without the ability of data encoding.

The chipless RFID tag presented in this chapter comprises two main components: UWB antenna and multiresonator. The multiresonating circuit consisted of cascaded spiral resonators which operate at different resonant frequencies. Each resonant frequency corresponded to a single data bit. The spiral resonator was chosen as the main encoding element since it exhibits compact size, high Q and small bandwidth in comparison to other planar resonators which exhibited stop-band performance.

Spectral signature encoding is used to encode data by the tag. Spectral signature requires a one to one (1:1) correspondence of the frequency spectrum behaviour to the tag's multiresonator layout. In particular, each spiral resonator had a 1:1 correspondence with a data bit, which meant that each data bit had a predetermined spiral resonant frequency. To the best of the author's knowledge, spectral signature encoding utilizing both amplitude and phase of the spectral signature is the first of its kind and has not been reported previously. The spiral resonance was represented by a null in the amplitude and abrupt jump in the phase which encoded logic "0". Encoding logic "1" was represented by the absence of an amplitude null and phase jump.

A fully novel "spiral shorting" concept of data encoding is presented in this thesis. The spiral resonator is shorted by shorting the spiral turns with a single trace. When shorted, the spiral resonator has a resonant frequency which is outside the operating band of the chipless RFID tag, hence resulting in the absence of the resonance. This is characterized as a logic "1" bit in the spectral signature. The removal of the shorting between the spiral turns introduces the resonance of the spiral resonator which is a representation of logic "0". This novel data encoding technique provides a new manufacturing advantage of the chipless RFID technology over other reported chipless RFID tags in terms of minimum layout modifications and the use of laser etching for mass tag encoding.

The design of the UWB monopole antennas for the chipless RFID tags was carried out. UWB disc-loaded monopole antennas exhibit omni-directional radiation patterns over their operating band and have an efficient and compact layout. The monopoles was designed using CPW technology as well.

The UWB chipless RFID system which utilizes a fully printable chipless CPW RFID tag which can be used for tracking low cost items such as banknotes, envelopes and other paper/plastic products, items and documents has been tested successfully. The chipless RFID tag operates between 5 and 10.7 GHz of the UWB spectrum. By exciting the tag with a wideband signal it was possible to detect variations in the magnitude and phase of the

received tag signal and decode the tag's ID at distances up to 70 cm in a noise-free environment and up to 35 cm in a laboratory (noisy) environment. It was necessary to calibrate the reader with a reference signature ID with no resonances when performing amplitude and phase data decoding.

Given the potential high demand on RFID technology in terms of reading range and applications some open issues and further areas of interest remain to be addressed in future projects. So far, the RFID tag has been designed to operate in predefined alignment situations and applications since the polarization of the antennas is crucial for successful reading. Further studies could focus on developing planar circularly-polarized tag antennas which would remove the present stringent alignment requirements. Another improvement which could be considered is making the tag operate with a single antenna instead of two which would dramatically reduce the size of the chipless tag. Further size reduction of the chipless tag can be achieved by using sub-millimetre-wave and millimetre-wave frequency bands. New applications for chipless tags (such as tram and train ticketing) could be established by extending the capacity of the chipless tags to 124 bits.

6. References

K. Finkenzeller (2003), "RFID Handbook - 2nd Edition", John Wiley & Sons, Ltd., 2003.

U. Kraiser, W. Steinhagen (1995), "A low-power transponder IC for high-performance identification systems", *IEEE Journal of Solid-State Circuits*, vol. 30, no. 3, pp:306-310, March 1995.

S. Preradovic, N. Karmakar (2009), "Modern RFID readers", *Microwave Magazine,* internet article, Available:<http://www.mwjournal.com/article.asp?HH_ID=AR_4830> (Accessed August 2009)

H. Stockman (2009), "Communication by Means of Reflected Power", Proceedings of the IRE, pp: 1196-1204, October 1948.

R. R. Fletcher (2002), "Low-cost electromagnetic tagging: design and implementation", PhD Thesis, September 2002. Available<www.media.mit.edu/physics/publications/theses/97.02.fletcher.pdf>

D. A. Hodges, H. G. Jackson (1998), "Analysis and design of digital integrated circuits – 2nd Edition", McGraw-Hill, New York, USA, 1988.

J. R. Baker, H. W. Li, D. E. Boyce, "CMOS circuit design, layout and simulation", IEEE Press, New York, USA, 1998.

S. Natarajan (2008), "A 32nm logic technology featuring 2nd –generation high-k + metal-gate transistors, enhanced channel strain and 0.171μm² SRAM cell size in a 291Mb Array", *IEEE International Electron Devices Meeting 2008 IEDM 2008*, pp:1-3, San Francisco, USA, 15-17 Dec. 2008.

S. Harma, V. P. Plessky, C. S. Hartmann, W. Steichen (2006), "SAW RFID tag with reduced size", *IEEE Ultrasonics Symposium 2006*, pp:2389-2392, Vancouver, Canada, Oct. 2006.

C. S. Hartmann (2002), "A global SAW ID tag with large data capacity", Reprint form *Proceedings of 2002 IEEE Ultrasonics Symposium*, vol. 1, pp:65-69, Munich, Germany, October, 2002, Available:http://www.rfsaw.com/pdfs/Global_SAW_ID_Tag_lg.pdf

R. Das, P. Harrop, Chip-less RFID forecasts, technologies & players 2006 – 2016, IDTechEx internet article, Feb.2006. <http://www.idtechex.com/products/en/view.asp?productcategoryid=96> (accessed March 2006)

S. Shretha, J. Vemagiri, M. Agarwal and K. Varahramyan (2007), "Transmission line reflection and delay-based ID generation scheme for RFID and other applications", *Int. J. Radio Freq. Identification Technol. Appl.*, vol. 1, no. 4, pp:401-416, 2007.

M. Glickstein (2006), Firewall protection for paper documents, RFID Journal internet article, Feb. 2004, <http://www.rfidjournal.com/article/articleprint/790/-1/1/>(accessed February 2006)

J. Collins (2004), RFID fibers for secure applications, RFID Journal internet article, March 2004. <http://www.rfidjournal.com/article/articleprint/845/-1/1/>(accessed April 2006)

K. C. Jones (2007), "Invisible tattoo ink for chipless RFID safe, company says", EE Times white paper, October 2007 <http://eetimes.eu/industrial/196900063> (accessed June 2009)

Jalaly, I. D. Robertson (2005), "RF barcodes using multiple frequency bands", *IEEE MTT-S International Microwave Symposium Digest 2005*, pp:4-7, Long beach, USA, June 2005.

J. McVay, A. Hoorfar, N. Engheta (2006), "Theory and experiments on Peano and Hilbert curve RFID tags", *Proceedings of the Wireless Sensing and Processing*, vol. 6248, pp:624808, San Diego, USA, Aug. 2006

Tagsense, Inc. (2006), "Chipless RFID products", data sheet, <http://www.tagsense.com/ingles/products/product_chipless.html> (accessed October 2006).

J. McVay, A. Hoorfar, N. Engheta (2006), "Space-filling curve RFID tags", *2006 IEEE Radio and Wireless Symposium*, pp: 199-202, San Diego, USA, 17-19 Jan. 2006.

Jalaly, D. Robertson (2005), "Capacitively-tuned split microstrip resonators for RFID barcodes", *2005 European Microwave Conference*, vol. 2 pp:4, Paris, France, 4-6 Oct. 2005.

S. Preradovic, I. Balbin, N. C. Karmakar, G. F. Swiegers (2009), "Multiresonator-based chipless RFID system for low-cost item tracking", *IEEE Transactions on Microwave Theory and Techniques,* vol. 57, no. 5, pp: 1411-1419, May 2009.

X. Chen, L. Guo, J. Liang, C. Parini (2007), "On the performance of UWB monopole antennas", *IEEE International Conference on Ultra-Wideband ICUWB 2007*, pp:210-213, Singapore, Sep. 2007.

A. Alipour, H. R. Hassani (2008), "A novel omni-directional UWB monopole antenna", *IEEE Transactions on Antennas and Propagation*, vol. 56, no. 12, pp: 3854-3857, Dec. 2008.

Q. Wu, J. Ronghong, J. Geng, M. Ding (2008), "Printed omni-directional UWB monopole antenna with very compact size", *IEEE Transactions on Antennas and Propagation*, vol. 56, no. 3, pp:896-899, March 2008.

G. Quintero, A. K. Skrivervik (2008), "Analysis of planar UWB elliptical dipoles fed by a coplanar stripline", *IEEE International Conference on Ultra-Wideband ICUWB 2008*, vol. 1, pp: 113-116, Hannover, Germany, Sep. 2008.

M. Mudroch, P. Cerny, P. Hazdra, M. Mazanek (2009), "UWB dipole antenna optimization with neural network tuned algorithm", *3rd European Conference on Antennas and Propagation EUCAP 2009,* pp:1491-1494, Berlin, Germany, March 2009.

G. Whyte, F. Darbari, I. McGregor, I. Glover, I. Thayne (2008), "Different feeding geometries for planar elliptical UWB dipoles, and the excitation of leakage current", *38th European Microwave Conference EuMC 2008*, pp:1382-1385, Amsterdam, Netherlands, Oct. 2008.

E.E. Angelopoulos, A. Z. Anastopoulos, D. I. Kaklamani, A. A. Alexandridis, F. Lazarakis, K. Dangakis (2006), "Circular and elliptical CPW-Fed slot and microstri-fed antennas for ultrawideband applications", *IEEE Antennas and Wireless Propagation Letters*, vol. 5, no. 1, pp:294-297, December 2006.

B.P. Wen (1969), "Coplanar waveguide: a surface strip transmission line suitable for nonreciprocal gyromagnetic device applications", *IEEE Transactions on Microwave Theory and Techniques*, vol. 17, no.12, pp:1087-1090, December 1969.

C. Hartmann, P. Hartmann, P. Brown, J. Bellamy, L. Claiborne, W. Bonner (2004), "Anti-collision methods for global SAW RFID tag system", *IEEE Ultrasonics Symposium*, vol. 2, pp:805-808, Montreal, Canada, August 2004.

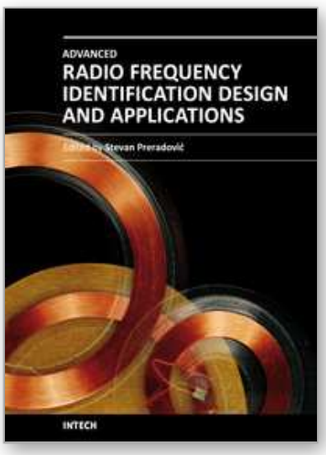

Advanced Radio Frequency Identification Design and Applications
Edited by Dr Stevan Preradovic

ISBN 978-953-307-168-8
Hard cover, 282 pages
Publisher InTech
Published online 22, March, 2011
Published in print edition March, 2011

Radio Frequency Identification (RFID) is a modern wireless data transmission and reception technique for applications including automatic identification, asset tracking and security surveillance. This book focuses on the advances in RFID tag antenna and ASIC design, novel chipless RFID tag design, security protocol enhancements along with some novel applications of RFID.

How to reference
In order to correctly reference this scholarly work, feel free to copy and paste the following:

Stevan Preradovic and Nemai Karmakar (2011). Fully Printable Chipless RFID Tag, Advanced Radio Frequency Identification Design and Applications, Dr Stevan Preradovic (Ed.), ISBN: 978-953-307-168-8, InTech, Available from: http://www.intechopen.com/books/advanced-radio-frequency-identification-design-and-applications/fully-printable-chipless-rfid-tag

INTECH
open science | open minds

InTech Europe
University Campus STeP Ri
Slavka Krautzeka 83/A
51000 Rijeka, Croatia
Phone: +385 (51) 770 447
Fax: +385 (51) 686 166
www.intechopen.com

InTech China
Unit 405, Office Block, Hotel Equatorial Shanghai
No.65, Yan An Road (West), Shanghai, 200040, China
中国上海市延安西路65号上海国际贵都大饭店办公楼405单元
Phone: +86-21-62489820
Fax: +86-21-62489821

IntechOpen